Analytical and Bioanalytical Chemistry (2022) 414:2089–2102
https://doi.org/10.1007/s00216-021-03843-1

RESEARCH PAPER

Structural characterization of phospholipids and sphingolipids by in-source fragmentation MALDI/TOF mass spectrometry

Hay-Yan J. Wang[1,2] · **Fong-Fu Hsu**[2]

Received: 17 August 2021 / Revised: 29 November 2021 / Accepted: 9 December 2021 / Published online: 11 January 2022

Abstract

Phospholipids (PLs) and sphingolipids (SLs) perform critical structural and biological functions in cells. The structure of these lipids, including the stereospecificity and double-bond position of fatty acyl (FA) chains, is critical in decoding lipid biology. In this study, we presented a simple in-source fragmentation (ISF) MALDI/TOF mass spectrometry method that affords complete structural characterization of PL and SL molecules. We analyzed several representative unsaturated lipid species including phosphatidylcholine (PC), plasmalogen PC (pPC), phosphatidylethanolamine (PE), phosphatidylinositol (PI), cardiolipin (CL), sphingomyelin (SM), and ceramide (Cer). Fragment ions reflecting the FA chains at sn–1 and sn–2 position, and those characteristics of the head groups of different PL classes, are readily identified. Specific fragment ions from cleavages of the C–C bond immediately adjacent to the *cis* C=C double-bond position(s) of FA chains and the *trans* C=C double bond of the sphingosine constituents allow precise localization of double bonds. The identities of the exemplary product ions from vinylic, allylic, and double-bond cleavages were also verified by LIFT-TOF/TOF. Identification of individual PL species in the lipid mixture was also carried out with ISF-MALDI/TOF. Together, this approach provides a simple yet effective method for structural characterization of PLs and SLs without the additional modification on the instrument hardware, and serves as a simple tool for the identification of lipids.

Keywords Phospholipids · Sphingolipids · Fatty acyl double-bond · MALDI/TOF · In-source fragmentation

Introduction

Lipids are widely distributed in all cells and organelles, playing critical roles as structural components and intercellular barriers, serving as important energy sources and second messenger in signal transduction, and performing many other cellular functions [1–4]. Phospholipids (PLs) and sphingolipids (SLs) contain both saturated and unsaturated fatty acyl (FA) chains with various double-bond positions and double-bond number that can affect their physical properties in the membrane bilayer [5, 6], influence the functions of neurotransmitter receptors [7], change the membrane fluidity [8] and the shape of ion channels in the mechanosensory transduction [9], and impact the gating of voltage-sensitive ion channels [10], leading to significant change in the physiological functions of the mammalian cells.

Total structural elucidation of lipid species, including lipid identity, stereospecificity, and the double-bond location of the FA chains are crucial in functional decoding of lipid biology under lipidomic workflow [11, 12]. Due to the high variability of double-bond location on the FA chain of these lipids, the number of isomeric structures can be numerous, and to distinguish their structures is a daunting task, despite that various mass spectrometric approaches have attempted to meet such demands. The conventional GC/MS method requires first release the FA chains from complex lipids, followed by derivatization to, e.g., fatty acid methyl esters (FAMEs) for GC/MS analysis. This approach gives limited information of the double-bond position of the FA chain, and its stereospecificity in the PL glycerol backbone, for

✉ Hay-Yan J. Wang
hyjwang@mail.nsysu.edu.tw

Fong-Fu Hsu
fhsu@im.wustl.edu

[1] Department of Biological Sciences, National Sun Yat-Sen University, Kaohsiung 80424, Taiwan

[2] Mass Spectrometry Resource, Division of Endocrinology, Diabetes, Metabolism, and Lipid Research, Washington University School of Medicine, Box 8127, St. Louis, MO 63110, USA

example, is lost [13]. By contrast, electrospray ionization (ESI) collision-activated dissociation (CAD) multiple stage mass spectrometry permits complete characterization of PLs and SLs, including the double-bond position of the FA chain [14, 15]. Several approaches including gas phase reaction applying ozone-induced dissociation (OzID) [16–19], UV-catalyzed Paternò-Büshi reaction [20–22], and UV photodissociation using 193-nm laser [23–26], coupled with MS or tandem mass spectrometry to define the double bond(s) of FA substituents in PLs and SMs, have been reported. On the other hand, hydrogen abstraction dissociation and oxygen attachment dissociation in tandem mass spectrometry [27], triboelectric nanogenerators coupled with time-aligned parallel fragmentation ion mobility mass spectrometry [28], or gas-phase charge transfer dissociation with high-energy helium cation beam [29] also have been employed for the study of lipid structures. However, these methods require specific instrument setups and modification that are not readily implementable in all laboratories.

Recently, we reported a simple in-source fragmentation (ISF)-MALDI/TOF mass spectrometry method for characterization of fatty acyl coenzyme A esters, revealing the double-bond position of the FA chain [30]. To explore the utility in the characterization of a broad range of lipid, we applied the same strategy to analyze several representative lipid species in PL and SL families. Here we reported the approach toward the structural identification of these lipids.

Materials and methods

Chemicals

All the PLs and SLs were purchased from Avanti Polar Lipids (Alabaster, AL, USA) or Sigma Chemical Co (St. Louis, MO, USA). Methanol (MeOH) and acetonitrile (ACN) were acquired from Fisher Scientific Co. 2-Propanol was acquired from VWR Chemicals BDH®. All the organic solvents used in this study were HPLC-grade or better. Water (18.2 MΩ) was produced in-house using a Millipore Milli-Q Reference A^+ Water Purification System. MALDI matrix 2,5-dihydroxybenzoic acid (DHB), 9-aminoacridine (9-AA), and sodium acetate (ACS-grade) were purchased from Sigma Chemical Co.

Sample preparation

Lipids used in this study were first prepared as 1 mg/mL stock solutions in MeOH, stored at − 20 °C, then diluted to 10–100 µg/mL in 60% MeOH as the lipid working solutions immediately before use. Ten microliters of lipid working solution was mixed with 7.5 µL DHB (30 mg/mL in 60% MeOH) or 9-AA (saturated solution in 60% 2-propanol/40% ACN (v/v) [31]) in an Eppendorf tube. Aliquots (1.2–1.5 µL) of lipid-matrix solution mixture were spotted on the stainless steel MALDI target plate and air dried. To enhance the formation of the sodiated adduct ions by MALDI, the lipid working solution can be mixed with 1 µL of 10 mM sodium acetate before mixing with the matrix solution.

Mass spectrometry

A Bruker Daltonics UltrafleXtreme MALDI/TOF/TOF mass spectrometer (Bremen, Germany) equipped with a Smartbeam-II™ laser was used for data acquisition. The MALDI/TOF and ISF-MALDI/TOF spectra were acquired in reflectron mode, either in the positive or negative ion mode depending on the sensitivity. The ionization voltage of Ion Source 1 and Ion Source 2 was set to 20 kV and 17.65 kV, respectively. The pulsed ion extraction (PIE) delay was 130 ns. The Smartbeam-II™ laser settings were set as follows: global attenuator offset: 20%, attenuator offset: 40%, attenuator range: 40%. The laser fluence was defined as 100% laser power minus laser beam attenuation, a parameter controlled by the instrument operator. The laser was operated at 500 Hz with a spot size set to "4_Large" for data acquisition. In MALDI/TOF data acquisition, lipids were ionized with laser fluence at 2–3% above threshold. In ISF-MALDI/TOF data acquisition, 1.5–2 times of threshold laser fluence was applied to induce in-source fragmentation. Ion signals from 2000 consecutive laser shots were summed into a spectrum in MALDI/TOF and ISF-MALDI/TOF acquisition. To acquire the MALDI LIFT-TOF/TOF spectra, 7.5 kV was applied to Ion Source 1, and 6.8 kV was applied to Ion Source 2, while the PIE delay was set to 90 ns. Each spectrum was an accumulation of ion signals over 10,000–12,000 laser shots.

Data processing and presentation

The MALDI spectra were first visualized using FlexAnalysis (version 3.4, Bruker Daltonics), then converted to mzXML format. Subsequent conversion of spectra to TIFF image files was carried out using mMass open source mass spectrometry program (version 5.5.0) [32, 33]. The signal-to-noise (S/N) ratio of 3 was defined as the peak identification threshold. To address the orientation of the FA chain, we defined the carboxyl terminal as the proximal end, and the opposite methyl terminal as the distal end. The C–C bond cleavages immediately distal to the double bond were defined as vinylic cleavages, while those immediately proximal to the double bonds were defined as allylic cleavages [30]. PL

and SL nomenclatures are according to the updated LIPID MAPS classification system [34].

Results

Phospholipid analyses in positive ion mode

Diacyl phosphatidylcholines

1-Palmitoyl-2-oleoyl-sn-glycero-3-phosphocholine (PC 16:0/18:1) We first applied a near-threshold laser energy (2–3% above the threshold) to obtain the MALDI/TOF MS spectrum. As expected, the spectrum of PC 16:0/18:1 (Supplementary Fig. S1) was dominated by ions of *m/z* 760.6 and 782.6, corresponding to the $[M+H]^+$ and $[M+Na]^+$ ions, respectively. Ions from prompt fragmentation were absent.

We then obtained the MALDI LIFT-TOF/TOF spectrum of protonated PC 16:0/18:1 ion at *m/z* 760.6. Not surprisingly, the spectrum was dominated by the phosphocholine ion at *m/z* 184.1 (Supplementary Fig. S2), along with ions of *m/z* 496.3 and 478.3 arising from loss of the 18:1 FA chain as ketene and acid, respectively, as well as ions of *m/z* 522.4 and 504.4, arising from the analogous loss of 16:0 FA chain. The spectrum also contained the *m/z* 577.5 ion, arising from loss of phosphocholine, but fragment ions associated with the cleavage of the C=C bond on the 18:1 FA chain were absent.

However, when the spectrum was obtained by ISF-MALDI/TOF (Fig. 1a), ions at *m/z* 760.6 ($[M+H]^+$), 782.6 ($[M+Na]^+$), and 798.5 ($[M+K]^+$) became dominant and the ion at *m/z* 184.1 was much less abundant than that in Figure S2. The spectrum also contained ions at *m/z* 496.3 and *m/z* 522.4 with their respective analogous sodiated ions at *m/z* 518.3, and 544.4. The higher abundance of *m/z* 496.3 ion than that of *m/z* 522.4 denotes the stereospecificity of the 16:0 and 18:1 FA chains at sn–1 and sn–2, respectively [35]. More importantly, ion of *m/z* 650.5, arising from the vinylic cleavage of the C–C bond immediately distal to the C=C bond at n–9 of the 18:1 FA chain, was observed (marked in red in Fig. 1a). This cleavage was consistent with the presence of ions at *m/z* 672.5 and 688.5, arising from the similar vinylic cleavage of $[M+Na]^+$ and $[M+K]^+$ ions, respectively. Ions of *m/z* 636.5 (marked in green in Fig. 1a) and the analogous sodiated *m/z* 658.5 arising from double-bond cleavage, plus ion of *m/z* 622.5 arising from the cleavage of the C–C acyl bond immediately proximal to the C=C bond of $[M+H]^+$, were also observed. The ISF-mediated bond cleavages, i.e., the vinylic, double-bond, and acyl cleavages immediately proximal to the double-bond, were also observed in PC 18:1/16:0 with similar relative abundance to that in Fig. 1a.

To support the findings, the *m/z* 650.5 ion seen by ISF-MALDI/TOF was further subjected to LIFT-TOF/TOF analysis (Fig. 1b) which yielded ions of *m/z* 496.4 and 478.5 from loss of 10:0 FA chain as ketene and acid, respectively, at sn–2, and ions of *m/z* 412.3 and 394.3 arising from similar loss of 16:0 FA chain at sn–1, along with ion of *m/z* 467.5 arising from loss of phosphocholine head group. The result clearly demonstrates that the ion of *m/z* 650.5 represents PC 16:0/10:0, which was generated by the increased in-source laser irradiation, leading to the vinylic cleavage of double-bond. This unique ion from vinylic cleavage readily leads to the location of double bond of the FA chain.

PCs containing polyunsaturated fatty acyl chain To test the applicability of ISF-MALDI/TOF method in the characterization of PC with polyunsaturated fatty acyl (PUFA) substituent, PC 16:0/22:6, an n–3 PUFA PC, and PC 18:0/20:4, an n–6 PUFA PC, were subjected to the same analytical procedure.

As shown in Fig. 2a, the $[M+H]^+$ and $[M+Na]^+$ ions of PC 16:0/22:6 were observed at *m/z* 806.6 and 828.6, respectively. The spectrum also contained the ions at *m/z* 496.3/518.3 (protonated/sodiated ion pair; same below) and 568.4/590.4 arising from loss of 22:6 and 16:0 FA chains as ketenes, respectively. The ions of *m/z* 496.3/518.3 are more abundant than the respective ions in the *m/z* 568.4/590.4 ion pair, consistent with the notion that 22:6 and 16:0 FA substituents are located at sn–2 and sn–1, respectively. The vinylic cleavages of the C–C bond immediately distal to the C=C bond at n–3, n–6, n–9, n–12, n–15, and n–18 of the 22:6 FA substituent were seen at *m/z* 780.5, 740.5, 700.5, 660.5, 620.4, and 580.4, respectively (marked in red in Fig. 2a). The analogous sodiated ions that were 22 Da heavier arising from similar cleavages from the $[M+Na]^+$ ion were also observed (*m/z* values parenthesized in black in the structural inset). The double-bond cleavages at n–4, n–10, n–13, n–16, and n–19 of the same FA chain were seen at *m/z* 766.4, 686.5, 646.4, 606.4, and 566.4, respectively (marked in green in Fig. 2a). The allylic cleavages of the C–C bond immediately proximal to the C=C bond at n–5, n–8, n–11, n–14, and n–17 of 22:6 FA were seen at *m/z* 756.5, 716.5, 676.5, 636.4, and 596.4, respectively (marked in blue in Fig. 2a). The n–20 acyl bond cleavage that yielded *m/z* 552.4 ion was also noted. The presence of these ions readily locates the double bonds at n–3, n–6, n–9, n–12, n–15, and n–18 of the 22:6 FA substituent.

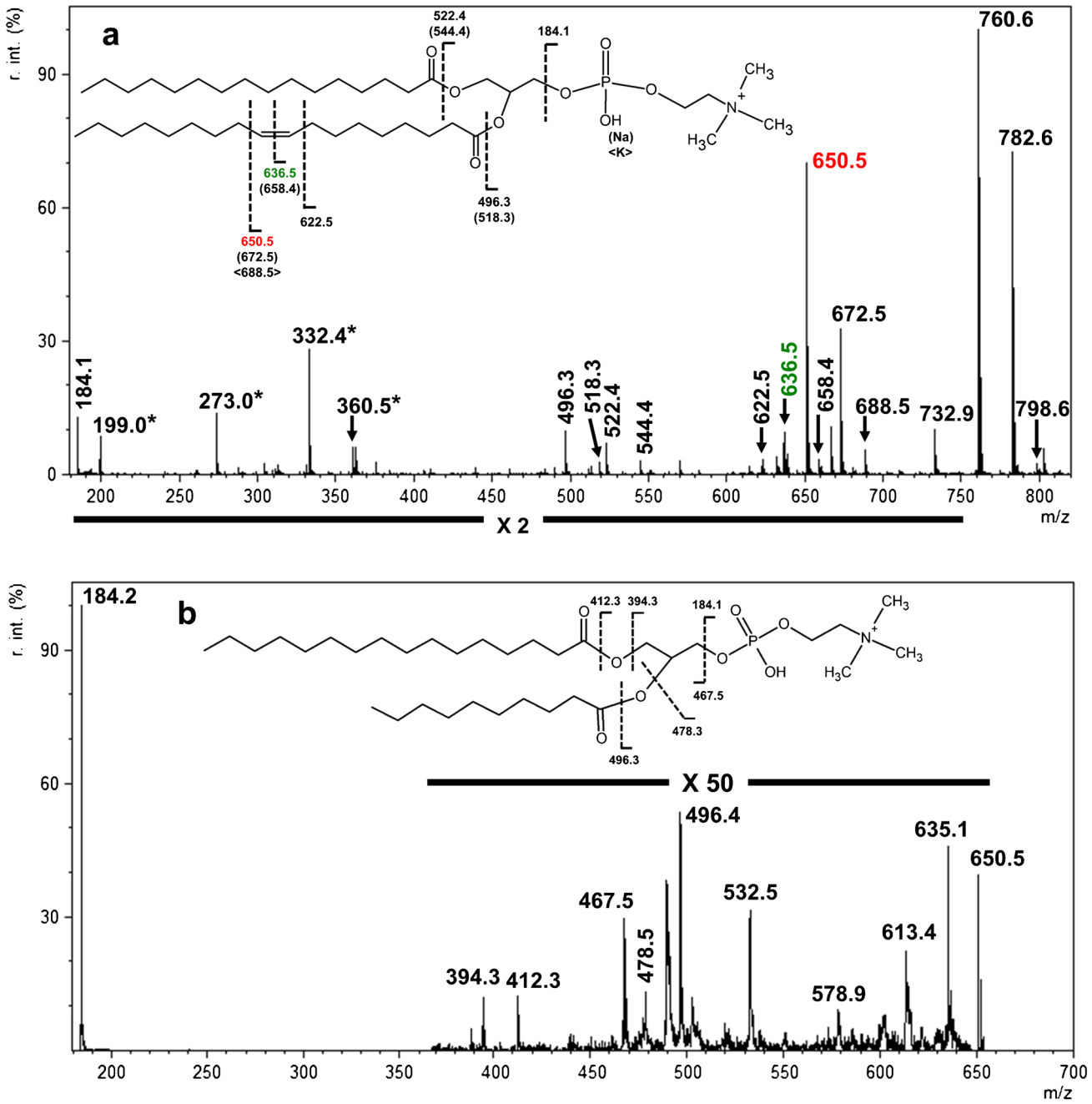

Fig. 1 ISF-MALDI/TOF of PC 16:0/18:1 and LIFT-TOF/TOF verification of its product ion from the vinylic cleavage. **a** ISF-MALDI/TOF spectrum of PC 16:0/18:1. Protonated ions of vinylic and double-bond cleavages of PC 16:0/18:1 were marked in red and green respectively in the spectrum and the structure inset. The *m/z* values of sodiated and potassiated ions of vinylic cleavage were marked in parentheses (()) and chevrons (<>), respectively. The ion intensity between *m/z* 180 and 750 was amplified by 2-folds. **b** LIFT-TOF/TOF spectrum of *m/z* 650.5 ion in **a**. Ion intensity between *m/z* 370 and 650 was amplified by 50-folds. *Ions from the MALDI matrix DHB.

Similarly, ISF-MALDI/TOF spectrum of the n–6 PUFA PC 18:0/20:4 (Fig. 2b) contained the ions at *m/z* 810.6 and 832.6, representing $[M+H]^+$ and $[M+Na]^+$, respectively. The *m/z* 832.6 ion was much more abundant than that of the *m/z* 810.6 ion, because the additional Na^+ was added in the sample preparation to simplify the data presentation. The spectrum also contains the ions at *m/z* 546.4 and 566.3, arising from loss of 20:4 and 18:0 FA chains as ketenes, respectively. Again, the ion at *m/z* 546.4 is more abundant than that at *m/z* 566.3, indicating that the 20:4 and 18:0 FA substituents are located at sn–2 and sn–1, respectively. The ions at *m/z* 764.5, 724.5, 684.5, and 644.4 (marked in red

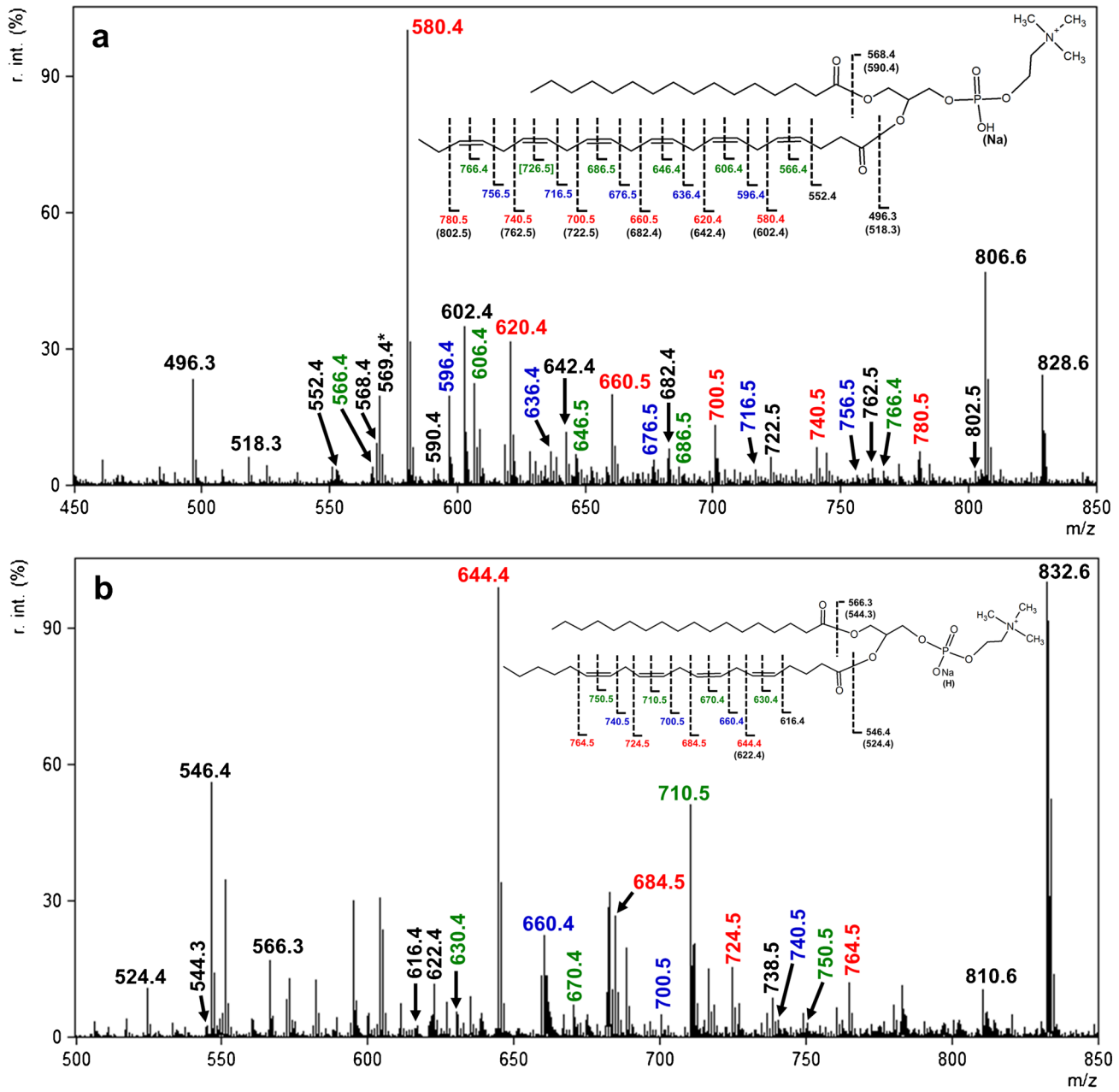

Fig. 2 ISF-MALDI/TOF spectra of PUFA-containing PCs. **a** ISF-MALDI/TOF spectrum of PC 16:0/22:6. Protonated product ions from vinylic, double-bond, and allylic cleavages were marked in red, green, and blue, respectively, in the spectrum and the structure inset. Parenthesized *m/z* values in the structure inset denoted the sodiated form, and the bracketed *m/z* value denoted undetected species. **b** ISF-MALDI/TOF spectrum of PC 18:0/20:4 with added Na^+ in preparation. Sodiated product ions from vinylic, double-bond, and allylic cleavages were marked in red, green, and blue, respectively, both in the spectrum and the structure inset. The *m/z* values of protonated ions were parenthesized in the structure inset.

in Fig. 2b) arising from vinylic cleavages of the C–C bond immediately distal to the C=C bond at n–6, n–9, n–12, and n–15 of the 20:4 FA chain, respectively, and ions of *m/z* 740.5, 700.5, and 660.4 (marked in blue in Fig. 2b) arising from the respective allylic cleavages of the C–C bond immediately proximal to the C=C bond at n–8, n–11, and n–14, of the 20:4 FA chain, while ions of *m/z* 750.5, 710.5, 670.4, and 630.4 from double-bond cleavages at n–7, n–10, n–13, and n–16 (marked in green in Fig. 2b) were also observed. The n–17 acyl bond cleavage which yielded the *m/z* 616.4 ion was also noted. These unique ions from the specific cleavages readily lead to the assignment of double-bond position

of the 20:4 FA substituent. The above results clearly demonstrate the utility of ISF-MALDI/TOF method in the structural characterization of PUFA-containing PC molecules, revealing the stereospecific positions of the FA chains and the locations of double bond.

Investigating product ions formed by allylic and double-bond cleavages To further investigate the FA chain composition after allylic and double-bond cleavages like those reported in "**PCs containing polyunsaturated fatty acyl chain**", we performed the LIFT-TOF/TOF analysis on an exemplary product ion arising from n–17 allylic cleavage at *m/z* 646.5 from sodiated PC 18:0/22:6. The spectrum in Fig. 3a revealed the *m/z* 587.4, 477.0, and 463.4 ions, representing the $[M+Na\text{-}59]^+$, $[M+Na\text{-}169]^+$, and $[M+Na\text{-}183]^+$ ions, respectively, together with fragment

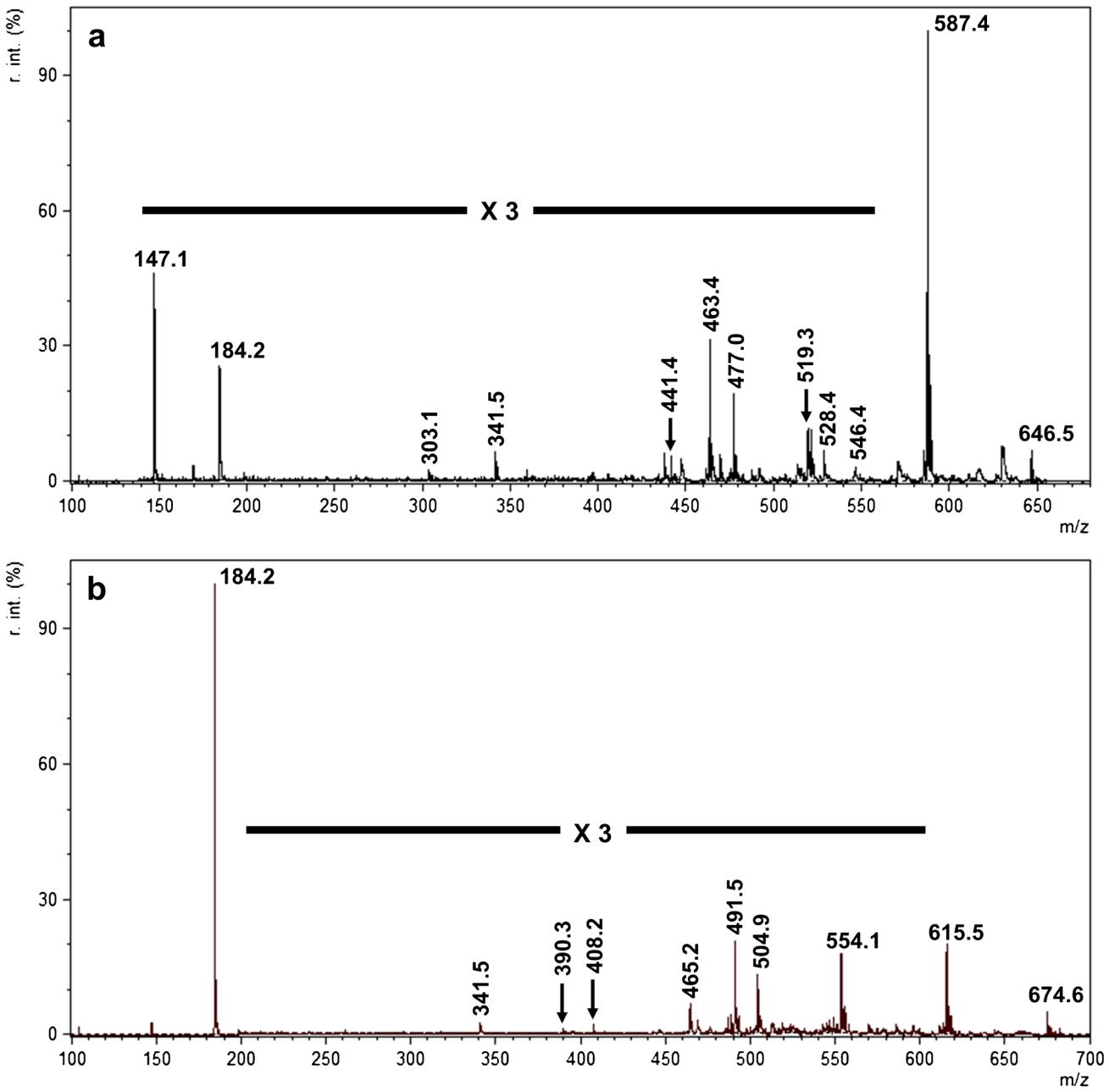

Fig. 3 LIFT-TOF/TOF analyses of product ions from allylic and double-bond cleavages of PC 18:0/22:6. **a** LIFT-TOF/TOF spectrum of sodiated n–17 allylic cleavage product ion at *m/z* 646.5 from PC 18:0/22:6 with added Na^+ in the preparation. Ion intensity from *m/z* 140 to 550 was amplified by 3-folds. **b** LIFT-TOF/TOF spectrum of protonated product ion from n–13 double-bond cleavage at *m/z* 647.6 from PC 18:0/22:6. Ion intensity from *m/z* 200 to 600 was amplified by 3-folds.

ions at *m/z* 147.0 ([phosphocholine + Na-59]$^+$) and the *m/z* 184.2 phosphocholine ion earmarked the phosphocholine head group features of the precursor ion. Ions from sn–2 loss as ketene and acid were detected at *m/z* 546.4 and 528.4, respectively, while the protonated [M+H-183-sn–2 ketene]$^+$ was detected at *m/z* 341.5. The spectrum also revealed the product ion of [M + Na-59-sn–1 18:0 acid]$^+$ at *m/z* 303.1. These product ions from sn–1 and sn–2 losses together support the notion that the sn–2 moiety of the n–17 allylic cleavage product of sodiated PC 18:0/22:6 contains $C_6H_{13}O$, confirming the presence of four additional hydrogen atoms by the allylic cleavage.

Using the same strategy, we investigated the characteristic product ion of n–13 double-bond cleavage at *m/z* 674.6 of protonated PC 18:0/22:6 (Fig. 3b). In addition to the phosphocholine ion at *m/z* 184.2, the LIFT-TOF/TOF spectrum also showed the [M + H-59]$^+$, [M + H-169]$^+$, and [M + H-183]$^+$ at *m/z* 615.5, 504.9, and 491.5, respectively. Furthermore, the spectrum revealed the product ion from sn–1 loss as ketene and acid at *m/z* 408.2 and 390.3, respectively. Product ion from the precursor ion losing the $N(CH_3)_3$ group together with the sn–2 moiety as ketene (i.e., [M + H-59-sn–2 ketene]$^+$) was detected at *m/z* 465.2, while a similar product ion from precursor ion losing the phosphocholine head group and the sn–2 moiety as ketene ([M + H-183-sn–2 ketene]$^+$) was seen at *m/z* 341.5. Characteristic product ions of precursor ions losing the respective sn–1 and sn–2 moiety support the notion that the sn–2 contains $C_{10}H_{15}O$, reflecting its similarity to the product ions of vinylic cleavage seen in Fig. 1b.

Other PLs

Plasmalogen To test the applicability of ISF-MALDI/TOF method beyond the diacyl PCs, we examined the plasmalogen PC 18:0/18:1 (pPC 18:0/18:1) using this method. The spectrum again contained the [M + H]$^+$ and [M + Na]$^+$ ions at *m/z* 772.6 and 794.6, respectively (Fig. 4a), and ions at *m/z* 522.4/544.4, arising from loss of the sn–1 alkenyl chain, and ions at *m/z* 550.4/572.4, arising from vinylic cleavage of the C–C bond immediately distal to the n–17 C=C bond of the C18 alkenyl chain, reflecting the presence of alkenyl chain at sn–1. The spectrum also contained ions at *m/z* 662.5/684.5, arising from cleavage of the C–C bond immediately distal to the C=C bond at n–9 of 18:1 FA chain at sn–2, consistent with the location of the double bond of the 18:1 FA chain at n–9, together with the phosphocholine ion at *m/z* 184.1 that confirmed the head group of this molecule. These results provide the double-bond positions both on the alkenyl chain at sn–1 and the unsaturated FA chain at sn–2 in a single spectrum, which, to the best of our knowledge, has not been described in any straight ESI-CAD spectra before. It is also interesting to note that fragment ions of *m/z* 522.4, 544.4, 550.4, and 572.4 were also detected in the MALDI/TOF spectrum at near-threshold laser fluence (Supplementary Fig. S3), likely due to the fact that plasmalogen phospholipids are labile.

1-Palmitoyl-2-docosahexaenoyl-sn-glycero-3-phosphoethanolamine (PE 16:0/22:6) To verify the utility of ISF-MALDI/TOF method in structural characterization beyond the PC class, we analyzed PE 16:0/22:6 mixed with Na^+ to enhance its ionization under positive ion mode. The spectrum (Fig. 4b) contained the [M + Na]$^+$ and the major [M-H + 2Na]$^+$ ions at *m/z* 786.5 and 808.5, respectively, together with ions at *m/z* 476.3/498.3 (monosodiated/disodiated pair; same below) and at *m/z* 548.3/570.3, arising from loss of 22:6 and 16:0 FA chains as ketenes, respectively. The ions in the former ion pair are more abundant than their respective counterparts in the latter pair, consistent with the notion that the 22:6 and 16:0 FA substituents are located at sn–2 and sn–1, respectively. The [M + H-141]$^+$ ion denoting the conventional signature neutral loss of the PE head group was detected at *m/z* 623.5, while ions at *m/z* 647.6 and *m/z* 669.5 likely arising from the loss of phosphoethanolamine head group unique to ISF-mediated fragmentation from the sodiated and disodiated PE 16:0/22:6 ions, respectively (Supplementary Fig. S4). Vinylic cleavages of the C–C bond immediately distal to the C=C bond at n–3, n–6, n–9, n–12, n–15, and n–18 of 22:6 FA chain of *m/z* 808.5 led to ions at *m/z* 782.4, 742.4, 702.4, 662.4, 622.3, and 582.3, respectively (marked in red in Fig. 4b). Double-bond cleavages at n–7, n–10, n–13, and n–16 of the same FA chain of *m/z* 808.5 resulted in *m/z* 728.4, 688.4, 648.4, and 608.3, respectively (marked in green in Fig. 4b). Allylic cleavages of the C–C bond immediately proximal to the C=C bond at n–5, n–8, n–11, n–14, and n–17 of 22:6 FA chain resulted in ions at *m/z* 758.4, 718.4, 678.4, 638.3, and 598.3, respectively (marked in blue in Fig. 4b). The *m/z* 554.3 from n–20 acyl bond cleavage was also detected. The results are consistent with those observed for PC 16:0/22:6 (Fig. 2a), readily locating the double-bond positions of the 22:6 FA chain at n–3, n–6, n–9, n–12, n–15, and n–18 of the sn–2 FA chain.

PL analyses in negative ion mode

1-Stearoyl-2-arachidonoyl-sn-glycero-3-phosphoinositol (PI 18:0/20:4) To further extend the applicability of ISF-MALDI/MS method, we examined PI 18:0/20:4 ionized under negative ion mode. As expected, the [M-H]$^-$ ion was seen at *m/z* 885.6 (Fig. 5a), together with ions at *m/z* 599.3 and 581.3, arising from loss of 20:4 FA chain as ketene and acid, respectively, and ions of *m/z* 619.3 and 601.3, arising from the corresponding loss of the 18:0 FA substituent.

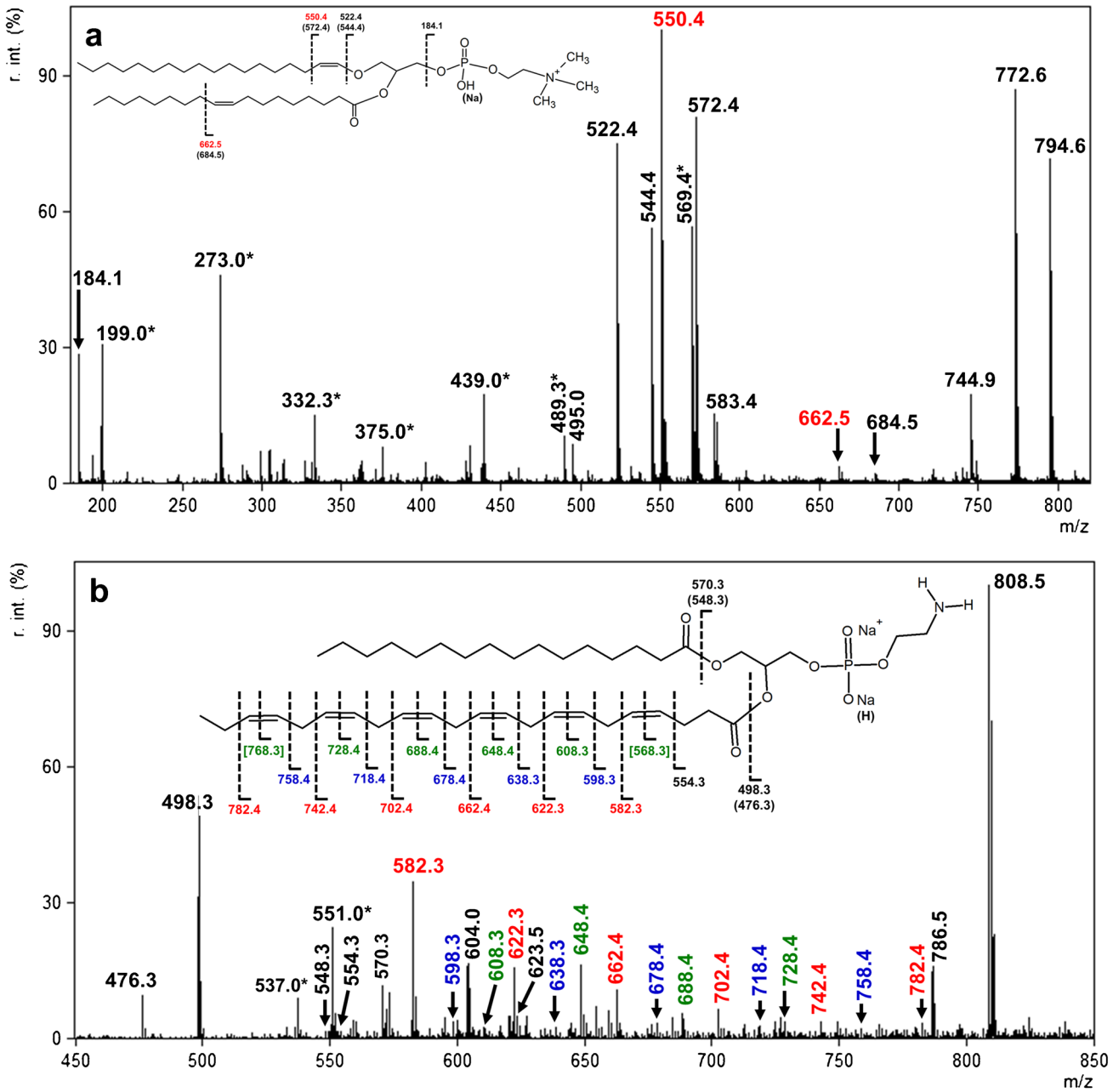

Fig. 4 ISF-MALDI/TOF spectra of other phospholipids in positive ion mode. **a** ISF-MALDI/TOF spectrum of plasmalogen PC (pPC) 18:0/18:1. Protonated product ions of vinylic cleavages were marked in red in the spectrum and the structure inset. Sodiated product ions of vinylic and other cleavages were parenthesized in the structure inset. **b** ISF-MALDI/TOF spectrum of PE 16:0/22:6 with added Na^+ in the preparation. The disodiated product ions from vinylic, double-bond, and allylic cleavages were marked in red, green, and blue, respectively, in the spectrum and the structure inset. The *m/z* values of monosodiated ions were parenthesized in the structure inset, while the bracketed *m/z* values denote undetected species. *Ions from the MALDI matrix DHB.

The ion abundance of the former ion pair was higher than that of the respective ions in the latter ion pair, indicating that the 20:4 and 18:0 FA substituents are located at sn–2 and sn–1, respectively [35]. Similar vinylic cleavages of the C–C bond immediately distal to the C=C bond at n–6, n–9, n–12, and n–15 of 20:4 FA chain resulted in product ions at *m/z* 817.5, 777.4, 737.4, and 697.4, respectively (marked in red in Fig. 5a). Double-bond cleavages at n–10, n–13, and n–16 led to the product ions at *m/z* 763.4, 723.4, and 683.4, respectively (marked in green in Fig. 5a). Allylic cleavages of the C–C bond immediately proximal to the C=C bond at n–8, n–11, and n–14, of 20:4 FA chain also yielded the product ions at *m/z* 793.4, 753.4, and 713.4, respectively (marked in blue in Fig. 5a). The *m/z* 669.4 from the acyl

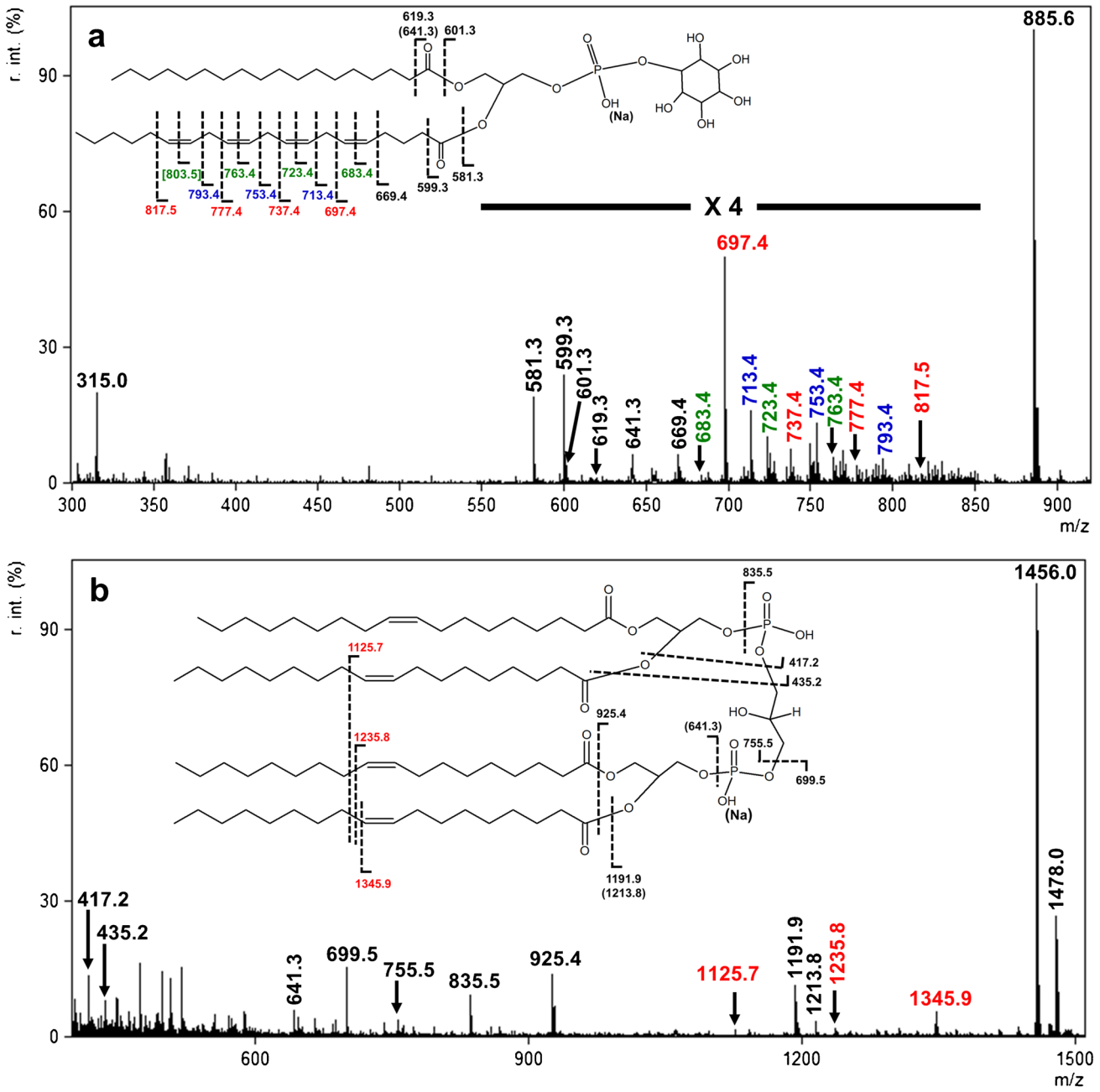

Fig. 5 ISF-MALDI/TOF spectra of phospholipids in negative ion mode. **a** ISF-MALDI/TOF spectrum of PI 18:0/20:4. Deprotonated product ions from vinylic, double-bond, and allylic cleavages were marked in red, green, and blue, respectively, in the spectrum and the structure inset. Parenthesized *m/z* value in the structure inset denoted the ion in $[M+Na-2H]^-$ form. Bracketed *m/z* value denoted the undetected ion species. Ion intensity between *m/z* 550 and 850 was amplified by 4-folds. **b** ISF-MALDI/TOF spectrum of cardiolipin $(18:1)_4$. Deprotonated product ions from vinylic cleavages were marked in red in the spectrum and the structure inset.

bond cleavage at n–17 was also observed. The spectrum also contained ion of *m/z* 315.0, a signature ion of PI [35]. The above structural information led to a complete characterization of the PI molecule desorbed as the $[M-H]^-$ ion.

1′,3′-bis[1,2-Dioleoyl-sn-glycero-3-phospho]-glycerol (cardiolipin 18:1) To probe the more complex PL structures, we obtained the ISF-MALDI/TOF spectrum of cardiolipin 18:1 (CL $(18:1)_4$) under negative ion mode. As was expected, both the major $[M-H]^-$ ion at *m/z* 1456.0 and the $[M+Na-2H]^-$ at *m/z* 1478.0 were observed (Fig. 5b). In the same spectrum, the ions at *m/z* 1191.9 and 925.4 arose from loss of one and two 18:1 FA chain as ketene, respectively, and ions of *m/z* 699.5 (a), 755.5 (a + 56), and 835.5 (a + 136) arising from

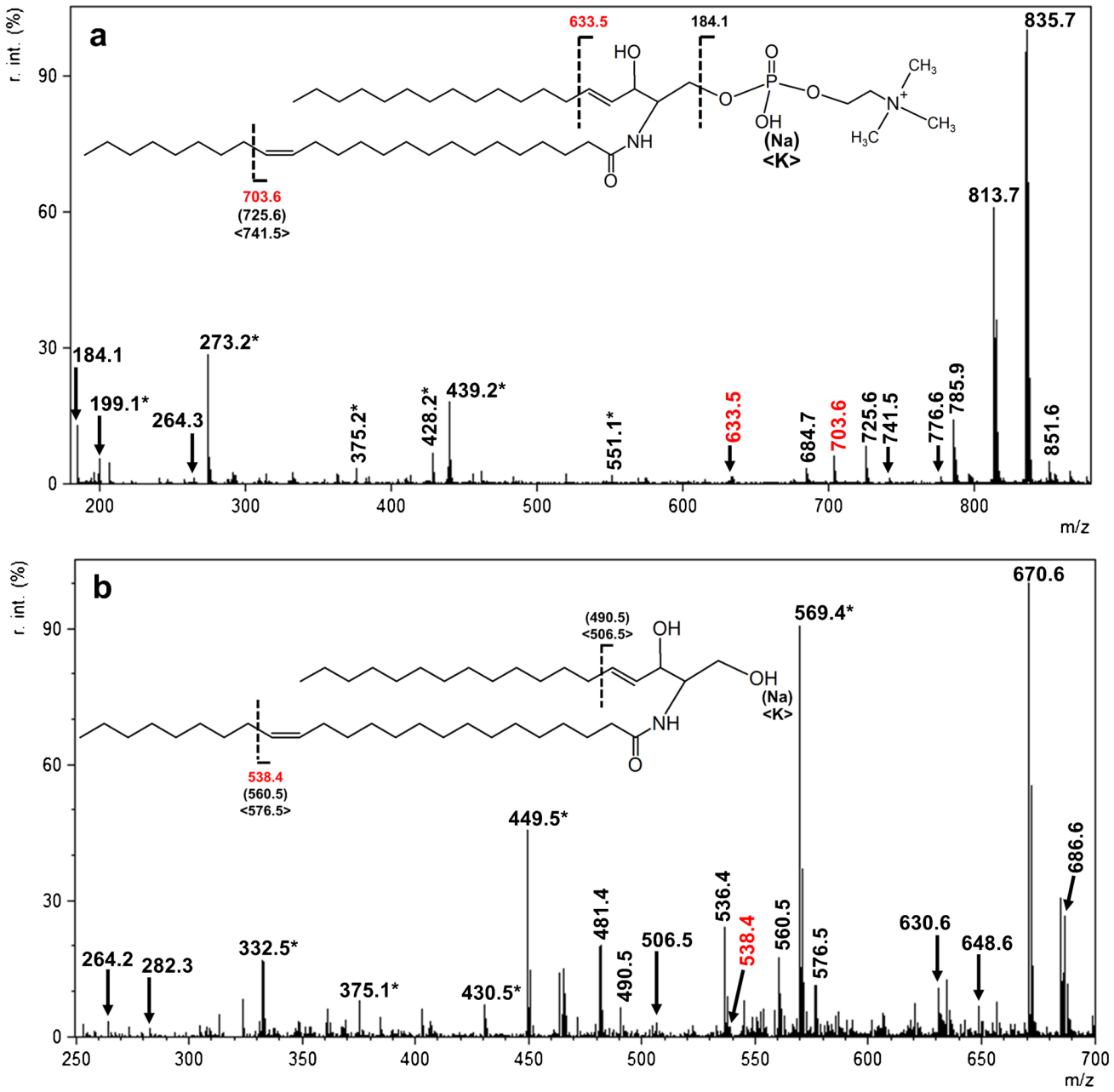

Fig. 6 ISF-MALDI/TOF spectra of sphingolipids. **a** ISF-MALDI/TOF spectrum of sphingomyelin d18:1/24:1. **b** ISF-MALDI/TOF spectrum of ceramide d18:1/24:1. Protonated ions of allylic cleavage were marked in red in the spectrum and the structure inset. Sodiated and potassiated ions of allylic cleavage were marked with parentheses and chevrons, respectively, in the structure inset. *Ions from the MALDI matrix DHB.

the fragmentation processes as previously described [36] were also present. The spectrum also contained the ions at *m/z* 1345.9, 1235.8, and 1125.7, arising from vinylic cleavages of the C–C bond immediately distal to the C=C bond at n–9 of one, two, and three of the four 18:1 FA substituents of the molecule, respectively (marked in red in Fig. 4b), indicating the location of the double bond on the 18:1 FA substituent at n–9. These structural information led to the assignment of $CL(18:1)_4$ structure. Such structural information including the double-bond position can otherwise be obtained only by MS^3 on the $[M\text{-}2H+3Li]^+$ ions in the positive ion mode with less sensitivity [37].

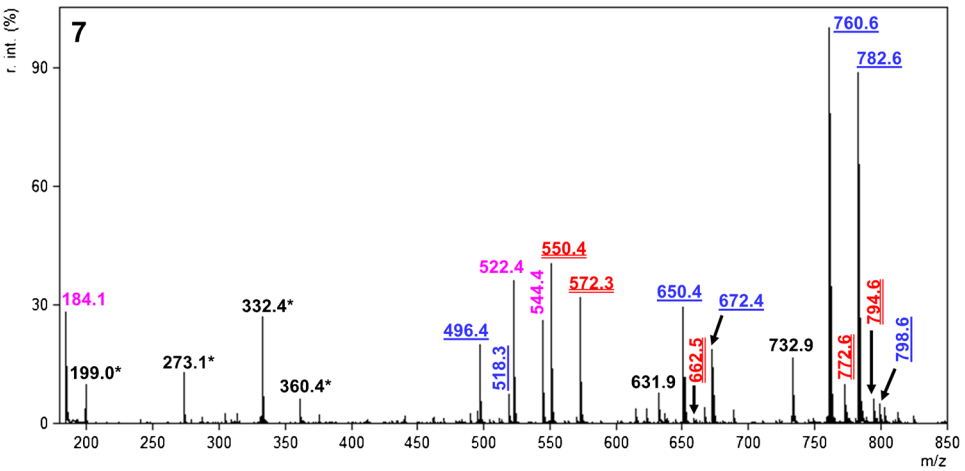

Fig. 7 ISF-MALDI/TOF spectrum of PC 16:0/18:1 and plasmalogen PC (pPC) 18:0/18:1 mixture at 5:1 molar ratio. Ions derived from PC 16:0/18:1 were marked in blue with single underline, and ions derived from pPC 18:0/18:1 were marked in red with double underline. Ions contributed by both phospholipid species were marked in pink. *Ion signals from the MALDI matrix DHB.

Sphingolipids

N-Nervonoyl-D-erythro-sphingosylphosphorylcholine (sphingomyelin d18:1/24:1) To extend the ISF-MALDI/TOF application beyond PL class, we applied this method to obtain the spectrum of sphingomyelin (SM) d18:1/24:1 (Fig. 6a). The spectrum revealed the $[M+H]^+$ and $[M+Na]^+$ ions at *m/z* 813.7 and 835.7, respectively, in addition to the *m/z* 184.1 that signifies the phosphocholine head group, and the *m/z* 264.3 ion that earmarks the d18:1-sphingosine long chain base (LCB) of SM [38]. The *m/z* 776.6 ion denotes the $[M+Na\text{-}59]^+$ ion derived from the sodiated precursor ion losing the $C(CH_3)_3$ head group. More importantly, the spectrum also contained the ion at *m/z* 703.6 (marked in red in Fig. 6a), arising from vinylic cleavage of the C–C bond immediately distal to the C=C bond at n–9 of the 24:1 FA chain, consistent with the observation of an analogous sodiated ion at *m/z* 725.6, arising from a similar cleavage of the $[M+Na]^+$ ion. This information affords the assignment of the C=C bond of the 24:1 FA chain at n–9. The low abundant *m/z* 633.5 ion (marked in red) arising from vinylic cleavage of the C–C bond immediately distal to the C=C bond on the LCB of the $[M+Na]^+$ ion also affords the assignment of n–14 *trans* double-bond on the sphingosine LCB.

N-Nervonoyl-D-erythro-sphingosine (ceramide d18:1/24:1) The ISF-MALDI/TOF spectrum of ceramide (Cer) d18:1/24:1 (Fig. 6b) showed this Cer ions in the forms of $[M\text{-}H_2O+H]^+$, $[M+H]^+$, $[M+Na]^+$, and $[M+K]^+$ at *m/z* 630.6, 648.6, 670.6, and 686.6, respectively, along with ions at *m/z* 264.2 and 282.3 that signify the sphingosine LCB in the molecule [38]. Again, the vinylic cleavage of the C–C bond immediately distal to the C=C bond at n–9 of the 24:1 FA chain yielded the *m/z* 538.4 fragment ion, consistent with the presence of the ions at *m/z* 560.5 and 576.5, corresponding to the sodiated and potassiated counterparts, respectively. These product ions of vinylic cleavages readily points to the double-bond position on the 24:1 FA chain at n–9 position. Vinylic cleavage of the C–C bond immediately distal to the *trans* C=C bond of the sphingosine from $[M+Na]^+$ and $[M+K]^+$ ion yielded the lower abundant *m/z* 490.5 and 506.5 ions, respectively, and located the double bond at n–14 of LCB. The simple ISF-MALDI/TOF method affords the assignment of both the double-bond positions of the LCB and the FA chain has not been previously described in the literature.

The results in both Fig. 6a and b show higher product ion abundance of ISF-mediated *cis* double-bond cleavage (*m/z* 703.6 in Fig. 6a; and *m/z* 538.4, 560.5, and 576.5 as protonated, sodiated, and potassiated product ions in Fig. 6b) than that of *trans* double-bond cleavage (*m/z* 633.5 in Fig. 6a; and *m/z* 490.5 and 506.5 as sodiated and potassiated product ions in Fig. 6b), when both the *cis* and *trans* vinylic cleavages were compared in the same spectrum.

PL mixture

To simulate the analytical scenario where lipid mixture is often encountered, we analyzed a mixture of PC 16:0/18:1 and pPC 18:0/18:1 at a molar ratio of 5:1 by ISF-MALDI/TOF (Fig. 7). The protonated, sodiated, and potassiated PC 16:0/18:1 ions, and their derived fragment ions from loss of sn–1 and sn–2 acyl moieties as ketenes, and ions from vinylic cleavage, were marked in blue with single underline (see "**1-Palmitoyl-2-oleoyl-sn-glycero-3-phosphocholine (PC 16:0/18:1)**" and Fig. 1a for reference). The ions of pPC 18:0/18:1 lineage were marked in red with double underline (see "**Plasmalogen**". and Fig. 3a for reference). Ions derived from both PC 16:0/18:1 and pPC 18:0/18:1, i.e., the protonated and sodiated LPC 18:1 at *m/z* 522.4 and 544.4, respectively, and the *m/z* 184.1 phosphocholine ion,

were marked in pink. The overall result indicates that ISF-MALDI/MS is capable of elucidating the structural features and the respective double-bond locations of PC 16:0/18:1 and pPC 18:0/18:1 in the mixture.

Discussion

Here, we demonstrated the utility of ISF-MALD/TOF method in the structural characterization of lipid species in the PL and SL families, including diacyl PC, plasmalogen PC, PE, PI, CL, SM, and Cer with various *cis* double bonds in the FA chain and *trans* double bond in the sphingosine, revealing the lipid class (i.e., the head group, LCB), the stereospecificity, and, more importantly, the double-bond position of the FA chain.

The phosphocholine fragment ion at *m/z* 184.1 observed in the ISF-MALDI/TOF spectra of PCs is significantly lower than that in the ESI-CAD product ion spectra, and in the MALDI LIFT-TOF/TOF spectra seen in this and previous studies [35, 39]. In contrast, the relative abundance of the fragment ions representing loss of the FA substituents at sn–1 or sn–2 as ketene are significantly higher. Such differences may be attributable to the higher internal energy imparted to the lipid molecular ions by the elevated laser fluence that overcomes a higher energy barrier for the ketene loss, leading to higher yields of product ions that are useful for the assignment of the stereospecificity of FA chains in PLs.

In the ISF-MALDI/TOF spectra, loss of FA substituents as ketenes is the predominant pathway, resulting in preferential loss of sn–2 FA ketene, similar to those previously observed in the CAD-MS/MS spectra of PLs [35]. This feature offers a reliable stereospecific assignment of the FA chains. However, applying exceedingly high laser fluence, e.g., over twice of the threshold fluence, for the ISF-MALDI/TOF MS process may lead to change in the pattern of FA-ketene loss, and result in inconclusive stereospecific assignment of the FA chains where hydrogen radical from hydroquinone-type acidic matrix [40–43] likely involves in the fragmentation process.

The present method is applicable to all forms of lipid molecular species, i.e., the protonated, sodiated, and potassiated species under positive ion mode, and the deprotonated, and the deprotonated alkali metal adduct ions under negative ion mode. This method is also applicable to different classes and subclasses of lipids such as PLs, SLs, and plasmalogen. Among all the bond cleavages, we noticed a prominent $[M+Na\text{-}139]^+$ fragment ion and the accompany $[M\text{-}H+2Na\text{-}139]^+$ fragment ion in the ISF-MALDI/TOF spectrum of PE 16:0/22:6 (Supplementary Fig. S4) apart from the $[M+H\text{-}141]^+$/$[M+Na\text{-}163]^+$ fragment ion commonly seen in the CAD-tandem mass spectra of PEs. We speculate that these ions may arise from a more energetic fragmentation process similar to that in previously reported for the ISD-cleavage of peptide bonds [41–43]. The loss of phosphoethanolamine head group may be initiated by the energized proton radicals generated by the ISF-MALDI process, forming the sodiated 1,2-O-diacyl propanediol (see the Supplementary Scheme). However, similar fragmentation processes were not seen in other PL families. Therefore, a systemic investigation to reveal the fragmentation process, which is beyond the scope of the current study, may be warranted.

The observation of the vinylic cleavage of the *trans* double bond in sphingosine backbone as seen in Cer and SM in addition to the *cis* double-bond cleavage in the SLs further supports that the ISF-MALDI/TOF method is also suitable for a complete structural determination of sphingolipids.

Compared to the product ions of vinylic and double-bond cleavages of FA chain, the allylic cleavages generate the truncated FA chains with one of the remaining double bonds saturated, which is quite different from those by the vinylic and double-bond cleavages. These observations were further verified by the subsequent MALDI LIFT-TOF/TOF analyses of the product ions from the ISF-mediated vinylic (Fig. 1b), allylic (Fig. 3a), and double-bond (Fig. 3b) cleavages.

The result of ISF-MALDI/TOF analyses of PL mixture indicates the necessity of coupling an upstream high-resolution separation or fractionation technique of PLs and SLs [44] to escalate the practicality of the current method. Proper separation that reduces the complexity of the sample mixture, and the combined analyses of ISF-MALDI/TOF and LIFT-TOF/TOF, will resolve most of the uncertainty in double-bond locations and the stereospecificity of the FA chains in most of the mixture scenario. Nevertheless, identification of PL species in the stereoisomer mixture, such as that of PC 18:0/18:1 and PC 18:1/18:0, by such coupled approach may become inconclusive unless an effective separation of the stereoisomers precedes the ISF-MALDI/TOF analyses, or a downstream structure-based separation of product ions by, e.g., ion mobility technique [45] is employed to verify the stereospecificity of the product ions.

When compared to other methods that define the double-bond positions and FA chain stereospecificity in lipids, we noticed that the product ions of the ISF-MALDI/TOF spectra from vinylic, allylic, and double-bond cleavages are more easily recognizable than those obtained by the OzID [16–19] or UVPD method [23–26] that requires significant instrument hardware modification. It is also worth to note that the present method is readily applicable for defining the stereospecificity of the FA chains, while the OzID and UVPD methods require additional MS^2 scans for the assignments. However, ISF-MALDI/TOF method encounters unpredictable relative abundance of the molecular and

fragment ions across the spectra when over 1 nmol of sample load is applied per spot. Another shortcoming of the present approach is the interference of the MALDI matrix, which can compromise data interpretation, in particular, when the sample load falls below 1 pmol per spot.

Another recently reported method that defines the FA double-bond positions, the UV-catalyzed Paternò-Büshi reaction coupled with tandem mass spectrometry (P-B method) [20–22, 46], proportedly reveals more structural information than that by OzID method. However, the P-B method also requires additional MS^2 scans for the assignment of FA chains. With the original molecular structures altered by the gas phase or liquid phase chemical reactions for locating the double-bond position, a more painstaking data interpretation is therefore required.

Conclusion

The ISF-MALDI/TOF method demonstrated herein is an effective approach that allows structural characterization of PLs and SLs, revealing the stereospecificity of the FA chains in PLs, the double-bond locations in the FA chain and the sphingosine LCB, and the lipid class-specific fragment ions, all in one single spectrum for structure characterization without a special instrument setup and modification. When coupled with proper separation techniques, this method may reach its full potential in structural characterization of these lipid families, and possibly other categories of lipids.

Supplementary Information The online version contains supplementary material available at https://doi.org/10.1007/s00216-021-03843-1.

Acknowledgements This study is sponsored by the Ministry of Science and Technology of Taiwan Grant No. MOST 108-2918-I-110-006 (H.Y.J.W.) and by the US Public Health Service Grants P41-GM103422 and P60-DK-20579. H.Y.J.W. would like to thank Prof. Amina S. Woods for her comments on the manuscript.

Declarations

Conflict of interest The authors declare no competing interests.

References

1. Harayama T, Riezman H. Understanding the diversity of membrane lipid composition. Nat Rev Mol Cell Biol. 2018;19(5):281–96. https://doi.org/10.1038/nrm.2017.138.
2. van Meer G, Voelker DR, Feigenson GW. Membrane lipids: where they are and how they behave. Nat Rev Mol Cell Biol. 2008;9(2):112–24. https://doi.org/10.1038/nrm2330.
3. Gross RW, Han X. Lipidomics at the interface of structure and function in systems biology. Chem Biol. 2011;18(3):284–91. https://doi.org/10.1016/j.chembiol.2011.01.014.
4. Casares D, Escriba PV, Rossello CA. Membrane lipid composition: effect on membrane and organelle structure, function and compartmentalization and therapeutic avenues. Int J Mol Sci. 2019;20(9):2167–96. https://doi.org/10.3390/ijms20092167
5. Martinez-Seara H, Rog T, Pasenkiewicz-Gierula M, Vattulainen I, Karttunen M, Reigada R. Effect of double bond position on lipid bilayer properties: insight through atomistic simulations. J Phys Chem B. 2007;111(38):11162–8. https://doi.org/10.1021/jp071894d.
6. Martinez-Seara H, Rog T, Pasenkiewicz-Gierula M, Vattulainen I, Karttunen M, Reigada R. Interplay of unsaturated phospholipids and cholesterol in membranes: effect of the double-bond position. Biophys J. 2008;95(7):3295–305. https://doi.org/10.1529/biophysj.108.138123.
7. Perillo VL, Fernandez-Nievas GA, Valles AS, Barrantes FJ, Antollini SS. The position of the double bond in monounsaturated free fatty acids is essential for the inhibition of the nicotinic acetylcholine receptor. Biochim Biophys Acta. 2012;1818(11):2511–20. https://doi.org/10.1016/j.bbamem.2012.06.001.
8. Yang X, Sheng W, Sun GY, Lee JC. Effects of fatty acid unsaturation numbers on membrane fluidity and alpha-secretase-dependent amyloid precursor protein processing. Neurochem Int. 2011;58(3):321–9. https://doi.org/10.1016/j.neuint.2010.12.004.
9. Ridone P, Grage SL, Patkunarajah A, Battle AR, Ulrich AS, Martinac B. "Force-from-lipids" gating of mechanosensitive channels modulated by PUFAs. J Mech Behav Biomed Mater. 2018;79:158–67. https://doi.org/10.1016/j.jmbbm.2017.12.026.
10. Boland LM, Drzewiecki MM. Polyunsaturated fatty acid modulation of voltage-gated ion channels. Cell Biochem Biophys. 2008;52(2):59–84. https://doi.org/10.1007/s12013-008-9027-2.
11. Porta Siegel T, Ekroos K, Ellis SR. Reshaping lipid biochemistry by pushing barriers in structural lipidomics. Angew Chem Int Ed Engl. 2019;58(20):6492–501. https://doi.org/10.1002/anie.201812698.
12. Lipidomics Standards Initiative Consortium. Lipidomics needs more standardization. Nat Metab. 2019;1(8):745–7. https://doi.org/10.1038/s42255-019-0094-z.
13. Peterson BL, Cummings BS. A review of chromatographic methods for the assessment of phospholipids in biological samples. Biomed Chromatogr. 2006;20(3):227–43. https://doi.org/10.1002/bmc.563.
14. Hsu FF, Turk J. Structural characterization of unsaturated glycerophospholipids by multiple-stage linear ion-trap mass spectrometry with electrospray ionization. J Am Soc Mass Spectrom. 2008;19(11):1681–91. https://doi.org/10.1016/j.jasms.2008.07.023.
15. Hsu FF. Complete structural characterization of ceramides as [M-H](-) ions by multiple-stage linear ion trap mass spectrometry. Biochimie. 2016;130:63–75. https://doi.org/10.1016/j.biochi.2016.07.012.
16. Ellis SR, Hughes JR, Mitchell TW, in het Panhuis M, Blanksby SJ. Using ambient ozone for assignment of double bond position in unsaturated lipids. Analyst. 2012;137(5):1100–10. https://doi.org/10.1039/c1an15864c.
17. Thomas MC, Mitchell TW, Blanksby SJ. Ozonolysis of phospholipid double bonds during electrospray ionization: a new tool for structure determination. J Am Chem Soc. 2006;128(1):58–9. https://doi.org/10.1021/ja056797h.
18. Mitchell TW, Pham H, Thomas MC, Blanksby SJ. Identification of double bond position in lipids: from GC to OzID. J Chromatogr B Analyt Technol Biomed Life Sci. 2009;877(26):2722–35. https://doi.org/10.1016/j.jchromb.2009.01.017.
19. Deeley JM, Thomas MC, Truscott RJ, Mitchell TW, Blanksby SJ. Identification of abundant alkyl ether glycerophospholipids in the

human lens by tandem mass spectrometry techniques. Anal Chem. 2009;81(5):1920–30. https://doi.org/10.1021/ac802395d.
20. Ma X, Xia Y. Pinpointing double bonds in lipids by Paterno-Buchi reactions and mass spectrometry. Angew Chem Int Ed Engl. 2014;53(10):2592–6. https://doi.org/10.1002/anie.201310699.
21. Stinson CA, Xia Y. A method of coupling the Paterno-Buchi reaction with direct infusion ESI-MS/MS for locating the C=C bond in glycerophospholipids. Analyst. 2016;141(12):3696–704. https://doi.org/10.1039/c6an00015k.
22. Franklin ET, Betancourt SK, Randolph CE, McLuckey SA, Xia Y. In-depth structural characterization of phospholipids by pairing solution photochemical reaction with charge inversion ion/ion chemistry. Anal Bioanal Chem. 2019;411(19):4739–49. https://doi.org/10.1007/s00216-018-1537-1.
23. Klein DR, Brodbelt JS. Structural characterization of phosphatidylcholines using 193 nm ultraviolet photodissociation mass spectrometry. Anal Chem. 2017;89(3):1516–22. https://doi.org/10.1021/acs.analchem.6b03353.
24. Klein DR, Feider CL, Garza KY, Lin JQ, Eberlin LS, Brodbelt JS. Desorption electrospray ionization coupled with ultraviolet photodissociation for characterization of phospholipid isomers in tissue sections. Anal Chem. 2018;90(17):10100–4. https://doi.org/10.1021/acs.analchem.8b03026.
25. Macias LA, Feider CL, Eberlin LS, Brodbelt JS. Hybrid 193 nm ultraviolet photodissociation mass spectrometry localizes cardiolipin unsaturations. Anal Chem. 2019;91(19):12509–16. https://doi.org/10.1021/acs.analchem.9b03278.
26. Williams PE, Klein DR, Greer SM, Brodbelt JS. Pinpointing double bond and sn-positions in glycerophospholipids via hybrid 193 nm ultraviolet photodissociation (UVPD) mass spectrometry. J Am Chem Soc. 2017;139(44):15681–90. https://doi.org/10.1021/jacs.7b06416.
27. Takahashi H, Shimabukuro Y, Asakawa D, Yamauchi S, Sekiya S, Iwamoto S, Wada M, Tanaka K. Structural analysis of phospholipid using hydrogen abstraction dissociation and oxygen attachment dissociation in tandem mass spectrometry. Anal Chem. 2018;90(12):7230–8. https://doi.org/10.1021/acs.analchem.8b00322.
28. Bouza M, Li Y, Wang AC, Wang ZL, Fernandez FM. Triboelectric nanogenerator ion mobility-mass spectrometry for in-depth lipid annotation. Anal Chem. 2021;93(13):5468–75. https://doi.org/10.1021/acs.analchem.0c05145.
29. Li P, Jackson GP. Charge transfer dissociation of phosphocholines: gas-phase ion/ion reactions between helium cations and phospholipid cations. J Mass Spectrom. 2017;52(5):271–82. https://doi.org/10.1002/jms.3926.
30. Wang HJ, Hsu FF. Revelation of acyl double bond positions on fatty acyl coenzyme a esters by MALDI/TOF mass spectrometry. J Am Soc Mass Spectrom. 2020;31(5):1047–57. https://doi.org/10.1021/jasms.9b00139.
31. Leopold J, Popkova Y, Engel KM, Schiller J. Recent developments of useful MALDI matrices for the mass spectrometric characterization of lipids. Biomolecules. 2018;8(4):173–97. https://doi.org/10.3390/biom8040173.
32. Strohalm M, Kavan D, Novak P, Volny M, Havlicek V. mMass 3: a cross-platform software environment for precise analysis of mass spectrometric data. Anal Chem. 2010;82(11):4648–51. https://doi.org/10.1021/ac100818g.
33. Strohalm M, Hassman M, Kosata B, Kodicek M. mMass data miner: an open source alternative for mass spectrometric data analysis. Rapid Commun Mass Spectrom. 2008;22(6):905–8. https://doi.org/10.1002/rcm.3444.
34. Fahy E, Subramaniam S, Murphy RC, Nishijima M, Raetz CR, Shimizu T, Spener F, van Meer G, Wakelam MJ, Dennis EA. Update of the LIPID MAPS comprehensive classification system for lipids. J Lipid Res. 2009;50(Suppl):S9-14. https://doi.org/10.1194/jlr.R800095-JLR200.
35. Hsu FF, Turk J. Electrospray ionization with low-energy collisionally activated dissociation tandem mass spectrometry of glycerophospholipids: mechanisms of fragmentation and structural characterization. J Chromatogr B Analyt Technol Biomed Life Sci. 2009;877(26):2673–95. https://doi.org/10.1016/j.jchromb.2009.02.033.
36. Hsu FF, Turk J, Rhoades ER, Russell DG, Shi Y, Groisman EA. Structural characterization of cardiolipin by tandem quadrupole and multiple-stage quadrupole ion-trap mass spectrometry with electrospray ionization. J Am Soc Mass Spectrom. 2005;16(4):491–504. https://doi.org/10.1016/j.jasms.2004.12.015.
37. Hsu FF, Turk J. Toward total structural analysis of cardiolipins: multiple-stage linear ion-trap mass spectrometry on the [M - 2H + 3Li]+ ions. J Am Soc Mass Spectrom. 2010;21(11):1863–9. https://doi.org/10.1016/j.jasms.2010.07.003.
38. Hsu FF, Turk J, Stewart ME, Downing DT. Structural studies on ceramides as lithiated adducts by low energy collisional-activated dissociation tandem mass spectrometry with electrospray ionization. J Am Soc Mass Spectrom. 2002;13(6):680–95. https://doi.org/10.1016/S1044-0305(02)00362-8.
39. Pridmore CJ, Mosely JA, Sanderson JM. The reproducibility of phospholipid analyses by MALDI-MSMS. Analyst. 2011;136(12):2598–605. https://doi.org/10.1039/c0an00436g.
40. Demeure K, Gabelica V, De Pauw EA. New advances in the understanding of the in-source decay fragmentation of peptides in MALDI-TOF-MS. J Am Soc Mass Spectrom. 2010;21(11):1906–17. https://doi.org/10.1016/j.jasms.2010.07.009.
41. Soltwisch J, Dreisewerd K. Discrimination of isobaric leucine and isoleucine residues and analysis of post-translational modifications in peptides by MALDI in-source decay mass spectrometry combined with collisional cooling. Anal Chem. 2010;82(13):5628–35. https://doi.org/10.1021/ac1006014.
42. Kocher T, Engstrom A, Zubarev RA. Fragmentation of peptides in MALDI in-source decay mediated by hydrogen radicals. Anal Chem. 2005;77(1):172–7. https://doi.org/10.1021/ac0489115.
43. Gao J, Cassady CJ. Negative ion production from peptides and proteins by matrix-assisted laser desorption/ionization time-of-flight mass spectrometry. Rapid Commun Mass Spectrom. 2008;22(24):4066–72. https://doi.org/10.1002/rcm.3818.
44. White T, Bursten S, Federighi D, Lewis RA, Nudelman E. High-resolution separation and quantification of neutral lipid and phospholipid species in mammalian cells and sera by multi-one-dimensional thin-layer chromatography. Anal Biochem. 1998;258(1):109–17. https://doi.org/10.1006/abio.1997.2545.
45. Rivera ES, Djambazova KV, Neumann EK, Caprioli RM, Spraggins JM. Integrating ion mobility and imaging mass spectrometry for comprehensive analysis of biological tissues: a brief review and perspective. J Mass Spectrom. 2020;55(12):e4614. https://doi.org/10.1002/jms.4614.
46. Murphy RC, Okuno T, Johnson CA, Barkley RM. Determination of double bond positions in polyunsaturated fatty acids using the photochemical Paterno-Buchi reaction with acetone and tandem mass spectrometry. Anal Chem. 2017;89(16):8545–53. https://doi.org/10.1021/acs.analchem.7b02375.